Shape based pharmacokinetic fluorescence optical tomography

Omprakash Gottam[a], Naren Naik[a,b*], Sanjay Gambhir[c]

[a]Department of Electrical Engineering, Indian Institute of Technology Kanpur, Kanpur-208016, INDIA

[b]Center for Lasers and Photonics, Indian Institute of Technology Kanpur, Kanpur-208016, INDIA

[c]Department of Nuclear Medicine, Sanjay Gandhi Postgraduate Institute of Medical Sciences, Lucknow-226014, INDIA

Abstract

Pharmacokinetic analysis of optical fluorophore provides physiological information of the abnormalities in tissue. Compartment modeling of the fluorophore pharmacokinetics quantify the physiological changes in the tissue. We propose a shape based tomographic reconstruction of pharmacokinetic rates, concentrations and volume fractions of the fluorophore using the time varying near infra-red measurements. Radial basis function based parametric levelsets are used to represent the boundary of the spatially varying parameters of interest. A regularized Gauss-Newton filter based scheme is used reconstruct shape, pharmacokinetic rates, volume fractions and concentration parameters. Reconstruction results for tumor mimicking numerical phantom validate our proposed approach.

Keywords: Pharmacokinetics, compartment analysis, tomography, Gauss-Newton filter, image reconstruction

1. INTRODUCTION

Biological changes such as high permeability and angiogenesis[1,2] in the cancerous tissue affect the pharmacokinetics of injected fluorophores. Spatially varying pharmacokinetic rate analysis of optical fluorophores can capture physiological changes due to abnormalities. Imaging the spatial pharmacokinetic rates using near-infrared (NIR) measurements can be a potential tool for cancer diagnosis and drug monitoring. Indocyanine green (ICG) is a commonly used optical fluorophore for cancer detection studies.[3,4] Compartment analysis of ICG pharmacokinetics[5,6] extracts the physiological changes in tissue. In compartmental analysis, the region of interest is divided into virtual compartments, such as blood plasma compartment and (tissue) extracellular and extravascular space compartment (EES); the pharmacokinetic rates describe the transfer rate of fluorophore between plasma and EES compartments.

Previous studies of pointwise-reconstruction of spatially varying pharmacokinetic rates[5–7] using NIR measurements have used stochastic estimation methods such as the extended Kalman filter and its variants. To improve the computational tractability, and reduce the search space dimension, we propose shape based reconstruction of the pharmacokinetic rates which are represented via parameterized levelsets (PALS) with radial basis functions (RBF). In our work we use the Gauss-Newton filter[8,9] to reconstruct the pharmacokinetic parameters and concentrations.

In section 2, we describe the problem setting and the state variable model. Section 3 contains the reconstruction scheme followed by numerical results and conclusion in section 4 and 5 respectively.

2. PROBLEM DEFINITION

The injected fluorophore leaks into EES compartment at tumor location and emits light with varying intensity over time. The exchange and elimination of the fluorophore in the compartments is governed by the following coupled ordinary differential equation[10]

$$\begin{bmatrix} \dot{C}_e \\ \dot{C}_p \end{bmatrix} = \begin{bmatrix} -k_{ep}(r) & k_{pe}(r) \\ k_{ep}(r) & -(k_{pe}+k_{elm}) \end{bmatrix} \begin{bmatrix} C_e \\ C_p \end{bmatrix} \equiv \mathbf{K} \begin{bmatrix} C_e \\ C_p \end{bmatrix} \tag{1}$$

where $C_p \equiv C_p(r,t)$ (μM), $C_e \equiv C_e(r,t)$ (μM) are the concentrations of ICG in the plasma and EES

*nnaik@iitk.ac.in; Phone:+91 512 259 6518

compartment respectively, k_{pe} (s^{-1}) (respectively k_{ep} (s^{-1})) is the transfer rate of ICG from the plasma compartment to the EES compartment (respectively the transfer rate of ICG from the EES compartment to the plasma compartment), k_{elm} (s^{-1}) is the transfer rate at which ICG is eliminated from the region of interest. Let Θ_0 be the set of unknown parameters needed to be reconstructed; $\Theta_0 \equiv \{\underbrace{C_e^i(0), C_p^i(0), C_e^o(0), C_p^o(0)}_{\boldsymbol{C}}, \underbrace{k_{pe}^i, k_{ep}^i, k_{elm}^i, k_{pe}^o, k_{ep}^o, k_{elm}^o}_{\boldsymbol{k}}, \underbrace{v_e^i, v_e^o, v_p^i, v_p^o}_{\boldsymbol{v}}, \boldsymbol{\gamma}\}$.

Denoting Δ as the sampling interval, the discretized state equation corresponding to 1 is given by[6]

$$\begin{aligned} \begin{bmatrix} C_e(r,j+1) \\ C_p(r,j+1) \end{bmatrix} &= e^{\mathbf{K}\Delta} \begin{bmatrix} C_e(r,j) \\ C_p(r,j) \end{bmatrix} \\ &\equiv \begin{bmatrix} \tau_{11}(r) & \tau_{12}(r) \\ \tau_{21}(r) & \tau_{22}(r) \end{bmatrix} \begin{bmatrix} C_e(r,j) \\ C_p(r,j) \end{bmatrix} \end{aligned} \quad (2)$$

The relation between the time varying absorption coefficient $\mu_{a(x/m)f}(r,j)$ ($'x/m'$ refers to excitation or emission wavelength) of the injected fluorophore and the concentration at a particular time instant j is given by[6,11]

$$\mu_{a(x/m)f}(r,j) = ln10 \cdot \epsilon_{(x/m)} \cdot (v_p C_p(r,j) + v_e C_e(r,j)) \quad (3)$$

where $\epsilon_{(x/m)}$ is the extinction coefficient, v_p and v_e being the volume fractions of the plasma and EES repectively.

Levelset representation of the spatially varying pharmacokinetic parameters (k_ξ, with $\xi = ep, pe, elm$) is given by

$$k_\xi(r) = k_\xi^i H(\phi(r,\gamma)) + k_\xi^o (1 - H(\phi(r,\gamma))) \quad (4)$$

where k_ξ^i and k_ξ^o represent $k_\xi^i(r)$ values inside and outside the tumor region respectively. $H(\cdot)$ represents the Heaviside function, and $\phi(r,\gamma)$ a function whose zero level set represents the boundary of the tumor. γ represents a set of shape parameters that define the levelset. We use a radial basis function representation of the object boundary with compactly-supported parametric level sets.[12] Concentrations in different compartments, which are dependent on pharmacokinetic rates are also assumed to be piecewise constant inside and outside the tumor region. The volume fractions, v_e and v_p are large in tumor region[1,10,13] as compared to healthy region. Hence the concentrations and volume fractions can also be represented using levelsets. Using level-set representation of concentrations and volume fractions, equation 3 can be rewritten as

$$\begin{aligned} \mu_{a(x/m)f}(r,j) = ln10 \cdot \epsilon \cdot [&(C_e^i(j) v_e^i + C_p^i(j) v_p^i) H(\phi(r)) + \\ &(C_e^o(j) v_e^o + C_p^o(j) v_p^o)(1 - H(\phi(r)))] \end{aligned} \quad (5)$$

The discretized state equation at time instant $j+1$ can be written as

$$\begin{bmatrix} C_e^i(j+1) \\ C_p^i(j+1) \\ C_e^o(j+1) \\ C_p^o(j+1) \\ \boldsymbol{k} \\ \boldsymbol{v} \\ \boldsymbol{\gamma} \end{bmatrix} = \begin{bmatrix} T^i & 0 & 0 \\ 0 & T^o & 0 \\ 0 & 0 & I \end{bmatrix} \begin{bmatrix} C_e^i(j) \\ C_p^i(j) \\ C_e^o(j) \\ C_p^o(j) \\ \boldsymbol{k} \\ \boldsymbol{v} \\ \boldsymbol{\gamma} \end{bmatrix} \quad (6)$$

where $T^{i/o} = \begin{bmatrix} \tau_{11}^{i/o}(\boldsymbol{k}) & \tau_{12}^{i/o}(\boldsymbol{k}) \\ \tau_{21}^{i/o}(\boldsymbol{k}) & \tau_{22}^{i/o}(\boldsymbol{k}) \end{bmatrix}$ and I is the identity matrix.

The measurement equation can be formally written as

$$y = \mathcal{G}(\Theta_0) \quad (7)$$

where y represents the vector of measurements and $\mathcal{G}(\cdot)$ represents the measurement operator; in our case it is evaluated using the finite element method (FEM) for the solution of the governing fluorescence diffusion model.[14]

3. RECONSTRUCTION

Reconstruction of this dynamic problem can be accomplished using stochastic methods like extended Kalman filter[6,7] (EKF) or deterministic methods like Gauss-Newton[8] (GN) filter. We employ the GN filter for reconstructing the unknown parameters. Letting g be the discretized version of $\mathcal{G}$ and f denoting the nonlinear state transition function, the measurement equation at time instant j is given by

$$\begin{aligned} y_j &= g_j(\Theta_j) \\ &= g_j(f_{j-1}(\ldots f_0(\Theta_0)\ldots)) \end{aligned} \quad (8)$$

where Θ_j is the parameter set at the time instant j.

The state variable model (6), (7)and (8) can be solved for unknown Θ_0 by solving the following regularized nonlinear least squares problem[8]

$$\hat{\Theta}_0 = \underset{\Theta_0}{\operatorname{argmin}}\, \mathbb{F}(\Theta_0) = \frac{1}{2} \left\| (\mathbf{g}(\Theta_0) - \mathbf{y}) \right\|^2 + \tau R(\Theta_0) \quad (9)$$

where $R(\cdot)$ is the regularization functional and τ is the regularization parameter. Here we consider $R(\Theta_0) = \|\Theta_0 - c\|^2$, where c represents an apriori known constant vector. This nonlinear least squares problem can be solved by the Levenber-Marquardt method in a line search or trust region framework,[8,15] with the following update

$$(\mathbf{J}^T\mathbf{J} + \tau R''(\Theta_0) + \lambda I)p_{\Theta_0} = -(\mathbf{J}^T\mathbf{r} + \tau R'(\Theta_0)) \quad (10)$$

where the Jacobian (sensitivity matrix) is given as

$$\mathbf{J} = \begin{bmatrix} J_0 \\ \vdots \\ J_{M-1} \end{bmatrix} \quad (11)$$

where M denotes the number of time instants and

$$J_{j-1} = G_{j-1}[\Theta_{j-1}]F_{j-1}[\Theta_{j-1}] \dots F_0[\Theta_0] \quad (12)$$

where $G[\cdot]$ and $F[\cdot]$ are the Frechet derivatives of measurement and state transition functions respectively. In our work the updates is carried out in a trust region framework[15]

4. NUMERICAL STUDIES

We consider a computational domain of size 4×4 cm with the origin as the center of the domain. A point sources (10mW power, 100Mhz modulation frequency) is placed at the center of each of the four boundary edges of the domain. Eight detectors are placed on each side of the domain with spacing of 0.4 cm; the detectors are placed symmetrically on either side of the source on that edge. Measurements are taken for 40 time instants with a sampling interval of 5 sec. At each time instant one source (counter clockwise) is on and 32 readings are taken from the detectors. Complex log intensity[15] of 1280 emission fluence measurements are used for reconstruction. The homogeneous optical properties of the phantom are[16] : $\mu_{axi} = 0.031\ cm^{-1}$, $\mu_{ami} = 0.00415\ cm^{-1}$, $\mu'_{sx} = 10.95\ cm^{-1}$, $\mu'_{sm} = 9.29\ cm^{-1}$, $\tau = 0.56\ ns$, $\phi = 0.016$, $R_{x,m} = 0.431$, $\epsilon_x = 130000\ M^{-1}cm^{-1}$, $\epsilon_m = 11000\ M^{-1}cm^{-1}$.

We test the proposed scheme with two numerical phantom; P1 being a two object inhomogeneity phantom and P2 being a single bean shaped phantom. The pharmacokinetic rates of invasive ductal carcinoma[5] are used to obtain synthetic data. We assume 6.5 μM concentration of fluorophore is injected via bolus. For data generation we consider the plasma concentration at the first time instant to be 6.5 μM and 0 μM for EES compartment.

The data is generated using finer mesh discretized with 160801 nodes containing 320000 triangular elements. Noise is added to data for generating two data sets (39.07dB-P1D1, 33.05dB-P1D2) for two object phantom and two sets (39.17dB-P2D1, 33.46dB-P2D2) for bean phantom. Reconstruction is done using coarser mesh discretized with 1681 nodes containing 3200 triangular elements. All the simulations are done in Matlab ® 2014a.

Table 1 shows the parameter values reconstructed for datasets of two phantoms. Shape reconstruction results obtained using proposed scheme are shown in figure 1. Red line denotes the shape of true object. Blue line indicates the initial lecelset contour. Black line is the reconstructed contour. Figures 1 (a) and (b) show the shape reconstruction of the phantom P1 and 1 (c) and (d) that of phantom P2.

We observe from our results (in table 1 and figures 1 and 2) a good object localization and reasonably good reconstruction of the pharmacokinetic parameters, thus enabling a clear demarcation of the tumor region.

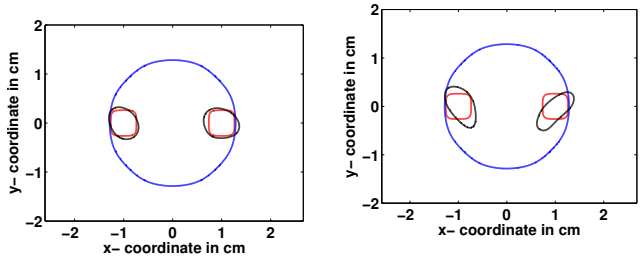

(a) (b)

Figure 1. Reconstruction of two object phantom for IDC tumor case. Red denotes the shape of true object, blue denotes the initial levelset and black denotes the reconstructed shape. (a)dataset PD1, (b) dataset PD2

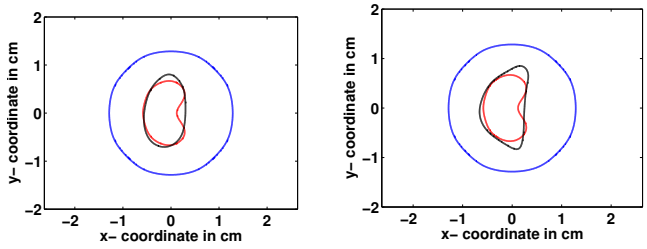

(a) (b)

Figure 2. Reconstruction of bean shape phantom for IDC tumor case. Red denotes the shape of true object, blue denotes the initial levelset and black denotes the reconstructed shape. (a)dataset P2D1, (b) dataset P2D2

Table 1. Pharmacokinetic parameters for Invasive ductal carcinoma Test case

Parameter	True values	P1D1	P1D2	P2D1	P2D2
C_e^i	0	1	1	1	1
C_p^i	6.5	6.5	6.5	6.5	6.5
C_e^o	0	0	0	0	0
C_p^o	6.5	6.5	6.5	6.5	6.5
k_{pe}^i	0.0687	0.0571	0.0583	0.0654	0.0535
k_{pe}^o	0.0306	0.0276	0.024	0.0228	0.0211
k_{ep}^i	0.0496	0.0217	0.0193	0.016	0.0188
k_{ep}^o	0.0166	0.0162	0.0133	0.0157	0.0179
k_{elm}^i	0.00449	0.0048	0.005	0.0037	0.0039
k_{elm}^o	0.00446	0.0044	0.0035	0.0038	0.0037
v_e^i	0.3	0.1044	0.1199	0.0989	0.0969
v_e^o	0	0	0	0	1.2×10^{-4}
v_p^i	0.06	0.07	0.07	0.07	0.0662
v_p^o	0.02	0.019	0.017	0.0166	0.0148

5. CONCLUSION

In this work, we propose a shape based dynamic tomographic reconstruction scheme for pharmacokinetic parameters using a regularized Gauss-Newton filter approach. The pharmacokinetic parameters, concentrations and volume fractions in a two compartment model are represented via an RBF based PALS representation. Numerical studies on tumor mimicking numerical phantoms are presented, that validate the proposed scheme. Our results show good localization and reasonable parameter reconstructions.

REFERENCES

[1] Cuccia, D. J., Bevilacqua, F., Durkin, A. J., Merritt, S., Tromberg, B. J., Gulsen, G., Yu, H., Wang, J., and Nalcioglu, O., "In vivo quantification of optical contrast agent dynamics in rat tumors by use of diffuse optical spectroscopy with magnetic resonance imaging coregistration," *Applied optics* **42**(16), 2940–2950 (2003).

[2] Hawrysz, D. J. and Sevick-Muraca, E. M., "Developments toward diagnostic breast cancer imaging using near-infrared optical measurements and fluorescent contrast agents1," *Neoplasia* **2**(5), 388–417 (2000).

[3] Ntziachristos, V., Yodh, A., Schnall, M., and Chance, B., "Concurrent mri and diffuse optical tomography of breast after indocyanine green enhancement," *Proceedings of the National Academy of Sciences* **97**(6), 2767–2772 (2000).

[4] Ishizawa, T., Fukushima, N., Shibahara, J., Masuda, K., Tamura, S., Aoki, T., Hasegawa, K., Beck, Y., Fukayama, M., and Kokudo, N., "Real-time identification of liver cancers by using indocyanine green fluorescent imaging," *Cancer* **115**(11), 2491–2504 (2009).

[5] Alacam, B., Yazici, B., Intes, X., Nioka, S., and Chance, B., "Pharmacokinetic-rate images of indocyanine green for breast tumors using near-infrared optical methods," *Physics in medicine and biology* **53**(4), 837 (2008).

[6] Alacam, B. and Yazici, B., "Direct reconstruction of pharmacokinetic-rate images of optical fluorophores from nir measurements," *IEEE transactions on medical imaging* **28**(9), 1337–1353 (2009).

[7] Wang, X., Zhang, Y., Zhang, L., Li, J., Zhou, Z., Zhao, H., and Gao, F., "Direct reconstruction in ct-analogous pharmacokinetic diffuse fluorescence tomography: two-dimensional simulative and experimental validations," *Journal of biomedical optics* **21**(4), 046007–046007 (2016).

[8] Naik, N., Beatson, R., and Eriksson, J., "Radial-basis-function level-set-based regularized gauss–newton-filter reconstruction scheme for dynamic shape tomography," *Applied optics* **53**(29), 6872–6884 (2014).

[9] Morrison, N., [*Tracking filter engineering: the Gauss-Newton and polynomial filters*], The Institution of Engineering and Technology (2012).

[10] Alacam, B., Yazici, B., Intes, X., and Chance, B., "Extended kalman filtering for the modeling and analysis of icg pharmacokinetics in cancerous tumors using nir optical methods," *IEEE transactions on biomedical engineering* **53**(10), 1861–1871 (2006).

[11] Landsman, M., Kwant, G., Mook, G., and Zijlstra, W., "Light-absorbing properties, stability, and

spectral stabilization of indocyanine green," *Journal of applied physiology* **40**(4), 575–583 (1976).

[12] Aghasi, A., Kilmer, M., and Miller, E. L., "Parametric level set methods for inverse problems," *SIAM Journal on Imaging Sciences* **4**(2), 618–650 (2011).

[13] Tofts, P. S., Brix, G., Buckley, D. L., Evelhoch, J. L., Henderson, E., Knopp, M. V., Larsson, H. B., Lee, T.-Y., Mayr, N. A., Parker, G. J., et al., "Estimating kinetic parameters from dynamic contrast-enhanced t 1-weighted mri of a diffusable tracer: standardized quantities and symbols," *Journal of magnetic resonance imaging* **10**(3), 223–232 (1999).

[14] Fedele, F., Laible, J., and Eppstein, M., "Coupled complex adjoint sensitivities for frequency-domain fluorescence tomography: theory and vectorized implementation," *Journal of Computational Physics* **187**(2), 597–619 (2003).

[15] Schweiger, M., Arridge, S. R., and Nissilä, I., "Gauss–newton method for image reconstruction in diffuse optical tomography," *Physics in medicine and biology* **50**(10), 2365 (2005).

[16] Eppstein, M. J., Fedele, F., Laible, J., Zhang, C., Godavarty, A., and Sevick-Muraca, E. M., "A comparison of exact and approximate adjoint sensitivities in fluorescence tomography," *IEEE Transactions on Medical Imaging* **22**(10), 1215–1223 (2003).